Ecology, 96(10), 2015, pp. 2758–2770

Can inducible resistance in plants cause herbivore aggregations? Spatial patterns in an inducible plant/herbivore model

Kurt E. Anderson,[1,3] Brian D. Inouye,[2] and Nora Underwood[2]

[1]*Department of Biology, University of California, Riverside, California 92521 USA*
[2]*Department of Biological Science, Florida State University, Tallahassee, Florida 32306 USA*

Abstract. Many theories regarding the evolution of inducible resistance in plants have an implicit spatial component, but most relevant population dynamic studies ignore spatial dynamics. We examined a spatially explicit model of plant inducible resistance and herbivore population dynamics to explore how realistic features of resistance and herbivore responses influence spatial patterning. Both transient and persistent spatial patterns developed in all models examined, where patterns manifested as wave-like aggregations of herbivores and variation in induction levels. Patterns arose when herbivores moved away from highly induced plants, there was a lag between damage and deployment of induced resistance, and the relationship between herbivore density and strength of the induction response had a sigmoid shape. These mechanisms influenced pattern formation regardless of the assumed functional relationship between resistance and herbivore recruitment and mortality. However, in models where induction affected herbivore mortality, large-scale herbivore population cycles driven by the mortality response often co-occurred with smaller scale spatial patterns driven by herbivore movement. When the mortality effect dominated, however, spatial pattern formation was completely replaced by spatially synchronized herbivore population cycles. Our results present a new type of ecological pattern formation driven by induced trait variation, consumer behavior, and time delays that has broad implications for the community and evolutionary ecology of plant defenses.

Key words: aggregations; herbivore population dynamics; induced resistance; plant–herbivore interactions; spatial pattern formation; time delays.

Introduction

Dynamic plant defenses against herbivory, termed inducible resistance, have received widespread attention since they were first described decades ago (Karban and Baldwin 1997, Tollrian and Harvell 1999, Karban 2011, Walters 2011). One major reason for deep interest in inducible resistance to herbivory is that it may affect the population dynamics of herbivores and thus alter patterns in herbivore damage. Convincing evidence exists that inducible resistance can affect herbivore performance and demographic traits such as births, growth, and survival (reviewed in Karban and Baldwin 1997). Both theoretical (Edelstein-Keshet and Rausher 1989, Lundberg et al. 1994, Underwood 1999, Abbott et al. 2008, Reynolds et al. 2013) and empirical (Underwood and Rausher 2002, Reynolds et al. 2012, Elderd et al. 2013) evidence suggests inducible resistance can indeed shape population dynamics of insects and small mammalian herbivores, and that induced plants accumulate less damage (Karban and Baldwin 1997, Thaler et al. 2001).

Manuscript received 3 September 2014; revised 21 January 2015; accepted 3 March 2015; final version received 2 April 2015. Corresponding Editor: S. J. Schreiber.
[3] E-mail: kurt.anderson@ucr.edu

Most population dynamic studies involving inducible resistance have focused on temporal fluctuations in herbivore abundances, ignoring spatial variability in these fluctuations. This is despite the fact that many theories regarding the evolution of inducible resistance have an implicit spatial component, as reviewed in Karban and Baldwin (1997), Agrawal and Karban (1999), and Zangerl (2003). A hypothesized benefit of inducible resistance is that it, coupled with herbivore movements, may create variance in damage among plants or plant parts, reducing damage to short bouts from which plants can easily recover. There is empirical evidence that insect herbivores move away from low quality plants and/or move up gradients in plant quality (Bernays and Chapman 1994), show feeding preferences for non-induced plants (Edwards et al. 1985, Cipollini et al. 2003, Kallenbach et al. 2012) and alter movement behavior within induced plants (Barker et al. 1995, Perkins et al. 2013). Yet whether these herbivore responses to induction alter larger scale spatial patterns remain unresolved. Edwards and Wratten (1983) proposed that insect herbivore movement away from areas of local induction should lead to even (dispersed) patterns of damage within a plant; this prediction can conceivably be extrapolated to apply to herbivore

movement and patterns of damage among plants. However, studies of patterns of insect damage among plants with inducible resistance have found damage ranging from dispersed to aggregated (Bergelson et al. 1986, Silkstone 1987, Underwood et al. 2005, Roslin et al. 2008, Viswanathan et al. 2008), defying simple generalization.

The implications of inducible defenses for herbivore spatial dynamics are likely to vary depending on the context and mechanism of induction; in this light, theory can provide guidance to when alternative patterns may emerge. A common theme in previous modeling studies is that the combination of nonlinear induction responses and time lags can drive temporal oscillations in the densities of insect herbivores and small herbivorous mammals (Lundberg et al. 1994, Underwood 1999, Abbott et al. 2008, Reynolds et al. 2012). Time lags in plant induction responses can arise in a number ways, including delays in the deployment of resistance, damage thresholds required for induction, and slow decay of induced traits, as seen in the examples in Underwood (1999) and Karban (2011). These in turn can delay the density dependent action of induction on herbivores, generating temporal instability. Lewis (1994) explored a model that included both variable plant quality and mobile herbivores and demonstrated that, when herbivores have strong tendencies to aggregate in areas of both high plant quality and high conspecific density, herbivores can show persistent spatial variation in density. However, Lewis (1994) did not include time lags and other features of inducible resistance shown to be important in nonspatial models. In contrast, Underwood et al. (2005) and Roslin et al. (2008) examined spatially explicit simulations that included time delays in induction. Their models predicted the possibility of herbivore aggregation in response to inducible resistance, which in turn led to aggregated patterns of damage among plants over time. Predicted patterns were supported empirically in both cases. However, the Underwood et al. (2005) and Roslin et al. (2008) models assumed fixed herbivore densities and analyzed limited subsets of key parameters. Hence, the limited modeling of induced resistance in a spatial context predicts an effect of induced resistance on spatial herbivore dynamics (see also Morris and Dwyer 1997), but with different mechanisms responsible for pattern formation in different models.

We explore the interplay between inducible resistance and herbivore spatial dynamics more generally using a collection of spatially explicit population dynamic models. These models extend and generalize both the nonspatial population dynamic model of Underwood (1999) and the spatially explicit behavioral simulations of Underwood et al. (2005) and Roslin et al. (2008). Our specific aim is to understand better how realistic features of plant inducible resistance and herbivore behavioral and demographic responses to such resistance affect the spatiotemporal dynamics of plant–herbivore systems. This model was constructed with herbivorous insects in mind, but should also apply to plants and small herbivorous mammals and other systems with inducible producer organisms and consumers that are numerous, small, and mobile (e.g., macroalgae and gastropod or isopod grazers; Long et al. 2007, Poore et al. 2014). We examine a novel mechanism where time delays in a plant's inducible resistance coupled with behavioral responses of herbivores to resistance levels lead to local instability and, hence, persistent spatial patterns. We also show how this mechanism may co-occur with other mechanisms known to generate oscillations in nonspatial models. To demonstrate key concepts in a simple context, we examine a hierarchy of models focused on basic mechanisms rather than attempt to model the details of a particular plant–herbivore system. However, it is also our objective to present an analytic formalism that can serve as the basis for a general, coherent theoretical framework describing the interactions between small consumers and producers with inducible resistance in a spatially explicit context.

Models of inducible resistance and herbivore dynamics

We use a system of differential equations to track the densities of herbivores and the level of inducible resistance in a linear array of discrete patches. Patches can represent a set of plant parts experiencing localized resistance (Orians et al. 2000, Perkins et al. 2013, Sarfraz et al. 2013), individual plants expressing systemic resistance, or plant aggregations linked by interplant communication (Karban et al. 2006), depending on the spatial scale of interest. Movements are therefore defined relative to what the patch represents; movements in the first case would be within or between nearby plants, while in the last case, they would be larger scale movements between clumps of plants or patches of forest. Resistance is treated, for ease of analysis, as either a single trait or an aggregate of traits that can be quantified by a single cumulative measure. Because the effects of inducible resistance on insect (Kaplan and Denno 2007) and small mammal (Reynolds et al. 2013) populations appear largely independent of plant biomass, we choose to model the dynamics of local inducible resistance levels without including plant growth or reproduction. In addition, focusing on induction levels allows the model to reflect empirical measurements of chemical resistance and herbivore feeding preference that are easily obtained via bioassay experiments, facilitating the confrontation between the model and data. We revisit this simplification in the *Discussion*.

The dynamics of induced resistance levels $I_j(t)$ and of herbivores $H_j(t)$ in a given patch j at time t are determined by the following equations:

$$\frac{dI_j}{dt} = \underbrace{\frac{\alpha H_{j,t-\tau}^{\theta}}{b^{\theta} + H_{j,t-\tau}^{\theta}}}_{\text{increase in induction}} - \underbrace{\delta I_j}_{\text{decay in induction}}$$

$$\frac{dH_j}{dt} = \underbrace{\rho(H_j)}_{\substack{\text{recruitment}\\ \text{of new}\\ \text{herbivores}}} - \underbrace{\gamma(I_j)H_j}_{\text{mortality}} - \underbrace{(d + \chi I_j)H_j}_{\text{emigration}}$$

$$+ \underbrace{\frac{1}{2}(d + \chi I_{j-1})H_{j-1} + \frac{1}{2}(d + \chi I_{j+1})H_{j+1}}_{\text{immigration}} . \qquad (1)$$

To minimize the influence of system boundaries, we assume that patches are far from any habitat edges. This scenario is approximated when necessary using periodic boundary conditions.

Changes in induction are dependent on herbivore densities τ, time steps in the past, denoted $H_{t-\tau}$, rather than on current herbivore densities to reflect the time it takes for most plants to synthesize and employ inducible defenses (e.g., Orians et al. 2000, Gomez et al. 2010, Karban 2011, Reynolds et al. 2012, Underwood 2012). While induced responses to repeated bouts of herbivory are not generally well characterized, there is evidence that resistance levels saturate with increasing damage (Underwood 2000, 2010, 2012, Stork et al. 2009, Reynolds et al. 2012). We assume that induced resistance increases in response to herbivore densities according to a saturating function, such that there is a maximum rate α by which induction can change after damage. The specific form of the herbivore effect function is determined by two parameters, θ and b. The parameter θ adjusts the shape of the function. When $\theta = 1$, the function decelerates monotonically, while $\theta > 1$ produces a sigmoidal shape, becoming a step function as $\theta \to \infty$. The parameter b is the half-saturation constant. Thus, increases in θ and b create a stronger threshold effect where low herbivore damage does not induce a strong resistance response (Underwood 2000, Massey et al. 2007). Induction levels decay at a constant per unit rate δ, reflecting the breakdown of inducible defenses and plant repair as well as inhibition by autotoxicity and nutrient limitation.

Herbivore spatiotemporal dynamics are determined by a mixture of movement, recruitment, and mortality. Herbivores possess two components of movement. The first is the baseline rate of emigration to a neighboring patch in the absence of induced resistance, which occurs with a per capita rate d. This is essentially a random movement term that represents the many factors besides induced resistance that influence movements and would typically be considered stochasticity in empirical measurements. The second component describes the increase in herbivore emigration rate as a function of induction level. The parameter χ is the increase in the per capita emigration rate per unit increase in induction. We assume that herbivores only respond to local conditions and do not exhibit any taxis towards neighboring patches possessing lower induction levels. Movements are defined relative to the size a patch represents, necessarily tying herbivore movement rates to these scales. For example, within-plant movements will typically occur more frequently than between-plant movements.

We examine different versions of Eq. 1, which we refer to as the open behavioral effect (hereafter OBE) model, the open behavioral and mortality effect (OBME) model, and the local behavioral and mortality effect (LBME) model. The models include different assumptions about herbivore recruitment and mortality that reflect different ecological conditions.

In the OBE model, we set $\rho = R$ and $\gamma = m$ for Eq. 1. For recruitment, we thus assume that herbivores arrive at a constant rate R from outside the system and that the per capita mortality rate m is initially independent of both herbivore density and induction level. This might be expected in a local plant population or agricultural field where new herbivores recruit from eggs laid by wide-ranging adults. The OBME model contains similarly open recruitment but with mortality that increases with increasing induction. This is achieved by setting $\gamma = \beta I_j$. The influence of mortality may reflect direct effects of toxicity or reduced nutritional content or indirect effects of increased predation risk (e.g., Thaler 2002, Kaplan et al. 2007). Finally, we examine a closed recruitment model, the LBME model, where herbivores reproduce and die locally. Herbivore population growth is logistic, $\rho = rH_j(1 - H_j/K)$, and inducible defenses reduce the net population growth rate at a constant per unit rate such that $\gamma = mI$ (Underwood and Rausher 2002).

These models possess a large number of parameters, which can obscure important mechanisms under a large amount of generated information. A standard workaround is dimensional analysis, which involves identifying a base unit for each parameter and then defining new parameters as ratios of the original parameters to their base units (Gurney and Nisbet 1998, Murray 2003). The resulting model is dimensionless and has fewer parameters, facilitating analysis.

We set our base unit for time as the average time it takes for induced resistance levels to decay, δ^{-1}, achieved by setting $\hat{t} = \delta t$. Our choice allows us to maintain a consistent and comparable parameterization even though herbivore recruitment and mortality terms vary among models. Because we are interested in the conditions that promote spatial patterning, we therefore scale induction levels, herbivore densities, and associated parameters by their expected average values at equilibrium, $\bar{I}^*$ and $\bar{H}^*$. In other words, herbivore densities and

induction levels are re-scaled to be one in all patches when spatial patterns are absent. The full details of our re-parameterization, including definitions for all nondimensional parameters, are presented in Appendix A. The resulting nondimensional OBE model is

$$\frac{d\hat{I}_j}{d\hat{t}} = (1+\hat{b}^{\theta})\frac{\hat{H}^{\theta}_{j,\hat{t}-\hat{\tau}}}{\hat{b}^{\theta}+\hat{H}^{\theta}_{j,\hat{t}-\hat{\tau}}} - \hat{I}_j$$

$$\frac{d\hat{H}_j}{d\hat{t}} = \hat{m}(1-\hat{H}_j) - (\hat{d}+\hat{\gamma}\hat{I}_j)\hat{H}_j + \frac{1}{2}(\hat{d}+\hat{\gamma}\hat{I}_{j-1})\hat{H}_{j-1} + \frac{1}{2}(\hat{d}+\hat{\gamma}\hat{I}_{j+1})\hat{H}_{j+1} \quad (2)$$

while the nondimensional OBME model is

$$\frac{d\hat{I}_j}{d\hat{t}} = (1+\hat{b}^{\theta})\frac{\hat{H}^{\theta}_{j,\hat{t}-\hat{\tau}}}{\hat{b}^{\theta}+\hat{H}^{\theta}_{j,\hat{t}-\hat{\tau}}} - \hat{I}_j$$

$$\frac{d\hat{H}_j}{d\hat{t}} = \hat{\beta}(1-\hat{I}_j\hat{H}_j) - (\hat{d}+\hat{\gamma}\hat{I}_j)\hat{H}_j + \frac{1}{2}(\hat{d}+\hat{\gamma}\hat{I}_{j-1})\hat{H}_{j-1} + \frac{1}{2}(\hat{d}+\hat{\gamma}\hat{I}_{j+1})\hat{H}_{j+1} \quad (3)$$

and the nondimensional LBME model is

$$\frac{d\hat{I}_j}{d\hat{t}} = (1+\hat{b}^{\theta})\frac{\hat{H}^{\theta}_{j,\hat{t}-\hat{\tau}}}{\hat{b}^{\theta}+\hat{H}^{\theta}_{j,\hat{t}-\hat{\tau}}} - \hat{I}_j$$

$$\frac{d\hat{H}_j}{d\hat{t}} = \hat{r}\hat{H}_j - (\hat{r}-\hat{\beta})\hat{H}_j^2 - \hat{\beta}\hat{I}_j\hat{H}_j - (\hat{d}+\hat{\gamma}\hat{I}_j)\hat{H}_j + \frac{1}{2}(\hat{d}+\hat{\gamma}\hat{I}_{j-1})\hat{H}_{j-1} + \frac{1}{2}(\hat{d}+\hat{\gamma}\hat{I}_{j+1})\hat{H}_{j+1}. \quad (4)$$

Hereafter, we drop hats for convenience and present variables and parameters as dimensionless quantities unless otherwise noted.

Model analyses

At the heart of our analyses, we ask whether small initial differences in induced resistance or herbivore aggregations between patches grow or decay (see Appendix B for details). Initial local differences could be perhaps seeded by hatchlings from egg clusters or by demographic or environmental stochasticity; these small initial differences grow into persistent spatial patterns in our models when the system is unstable, and attenuate when the system is stable. Mathematically, our analyses are accomplished by subjecting the average equilibrium induction level $\bar{I}^*$ or herbivore density $\bar{H}^*$ to a small, spatially variable perturbation and examining the resulting dynamics. In particular, we derive the perturbation growth rate, denoted ξ (see Appendix B), which provides the approximate rate at which spatial perturbations grow or decay. The perturbation growth rate is positive when the system is unstable and the perturbations grow into persistent spatial patterns, and is negative when the system is stable and initial spatial patterning decays.

Our analyses demonstrate that whether or not we see perturbations grow into spatial patterns in our model is often determined by the component spatial frequencies of the perturbation. While the spatial distribution of herbivores in any real ecological system will never be simple, we can still make significant progress by examining the perturbation growth rate across a range of different spatial frequencies k. Note that each spatial frequency k has a corresponding spatial wavelength $2\pi/k$, meaning that perturbations with high spatial frequencies vary over small spatial scales, while low frequencies vary over large scales. Frequencies that are unstable will grow and contribute to spatial patterns in herbivore densities or induced resistance levels, while those that are stable will tend to dissipate. In other words, we expect herbivore aggregations to form whose spatial scale reflects unstable spatial frequencies present in the initial perturbation.

Our analyses also demonstrate the key role that the induction time delay τ plays in herbivore aggregation (Appendix B). For any given set of model parameters that promote pattern formation, there will be a critical time delay τ_c that is required for patterns to form. When the induction time delay is longer than the critical delay, the system will be destabilized, leading to oscillations in induction levels and herbivore densities at each patch j that occur with temporal frequency ω. Because the initial perturbations to the system vary with spatial frequency k, temporal oscillations will not be synchronized across patches, causing wave-like spatial patterns to emerge. We further explore the relationship between model parameters, the scale of spatial perturbations, time delays, and spatial pattern formation in the results that follow.

Results

OBE model

Fig. 1 shows the relationship between stability, spatial frequency of perturbation k, and induction time delay τ for the OBE model. When there is no time delay in induction, the model is highly stable over all spatial frequencies k. In other words, spatial patterns will never form in the OBE model when there is no induction time delay (this result is demonstrated analytically in Appendix B). Variation in induction levels or herbivore densities will therefore quickly dissipate in the model. The model eventually loses stability over values of k larger than a critical value as the time delay increases. Larger values of the frequency k correspond to variability that occurs over the smallest scales, meaning that small-scale aggregations of herbivores (e.g., from a clutch of eggs) are most likely to be maintained. Once the model becomes unstable, larger values of the time

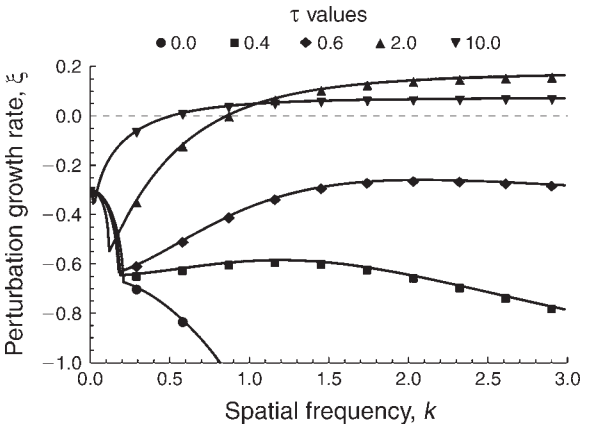

FIG. 1. The effect of the spatial frequency of an initial perturbation k and the induction time delay τ on the stability of the OBE (open behavioral effect) model, Eq. 2. Stability is determined by the perturbation growth rate ξ. When the perturbation growth rate is negative, the system is stable and tends toward uniform spatial equilibria. Positive values indicate instability and the formation of persistent spatial patterns in induced resistance levels and herbivore densities. Other parameter values are mortality rate, $\gamma = 0.3$; emigration sensitivity, $\chi = 2.0$; baseline emigration, $D = 0.1$; half-saturation constant, $b = 1.0$; and shape constant, $\theta = 5.0$.

delay increase the lower range of spatial frequencies that can lead to instability, meaning that larger spatial scales of variability in induction or herbivore densities can be sustained. As the range of unstable frequencies increases, the perturbation initially grows faster (i.e., the magnitude of perturbation growth rate ξ increases). However, it eventually decreases for very large time delays, albeit always staying positive. This simply reflects the increased time it takes for the eventual form of spatial patterns to develop when the induction time delay is very long.

Fig. 2 presents example spatiotemporal dynamics of the OBE model with different values of time delay τ. As shown in Fig. 1, the OBE model is highly stable when $\tau = 0$. Initial variation in herbivore densities causes transient spatial variation in inducible defenses, but heterogeneity in both herbivore densities and induction levels quickly dissipates. Spatial patterns persist much longer as the time delay is increased to 1.25. However, the model is still stable, meaning that the patterns eventually dissipate. Initial herbivore variation leads to variation in induction, with herbivores in turn quickly moving away from induction areas and aggregating in areas of low induction. As new herbivore aggregations lead to local increases in induction, herbivores quickly depart and aggregate in neighboring low-density areas where previously high induction levels have relaxed. The process is repeated, leading to aggregations of herbivores moving among patches over time. This spatiotemporal pattern is not sustained, eventually dampening until the system returns to its uniform steady state. Once the time delay is set to 2.5, it has surpassed the critical value τ_C and the model is no longer stable (for the parameter combination in Fig. 2, $\tau_C \approx 1.45$). Spatiotemporal patterns that dampened when $\tau = 1.25$ are now sustained. Over time, herbivores become more highly aggregated, moving from high to low induction areas in wave-like formations.

While the range of unstable spatial frequencies increases with increasing time delay (Fig. 1), the model will always be stable in the face of very large-scale perturbations. This is a consequence of inducible resistance affecting herbivore movement rates but not demographic rates. If the OBE model exhibited classic consumer–resource cycles driven by feedbacks of induction on herbivore demographic rates, we would expect the system to oscillate when induction or herbivore densities are perturbed evenly across all patches. Instead, the OBE model is always stable in the face of such global perturbations and does not even exhibit transient oscillations (Fig. 1; Appendix B). It is only at the smaller scales, where herbivores react to variation in induction through movement, where spatial patterns can develop.

Using analyses outlined in Appendix B, we arrive at the conclusion that the OBE will be unstable, leading to the formation of spatial patterns, when

$$\Lambda = \frac{\theta b^{\theta}}{1 + b^{\theta}} - \frac{2m}{\chi k^2} - \frac{d}{\chi} - 1 \geq 0. \tag{5}$$

We refer to Λ as the instability metric. The influence of parameters in promoting or inhibiting instability can be deduced from examining Eq. 5. Fig. 3 presents the relationship between different parameters and instability, as measured by the criterion Eq. 5, and the corresponding time delay required for instability.

First, the movement sensitivity of herbivores to induction levels χ increases the potential of the model to lose stability and therefore patterns to arise. As the sensitivity increases, the system can lose stability given a sufficient time delay, and the value of this time delay required for instability decreases as χ increases (Fig. 3a). When herbivores become increasingly sensitive to induction levels in their patch, their resulting high-movement rates mean that they take less time to leave these patches and find others with lower induction. Indeed, some level of herbivore movement sensitivity is always required for spatial patterns to develop (Appendix B).

The random component of movement d has an opposite, stabilizing effect. With higher d, a greater level of movement sensitivity χ is required to destabilize the system. Random movement has a well-known stabilizing effect because it works to smooth out variation in density, especially over small spatial scales, by efficiently moving herbivores in areas of high densities to areas of low densities. Movement sensitivity needs to be greater when random movement is higher to overcome this effect and aggregate herbivores in areas of low induction.

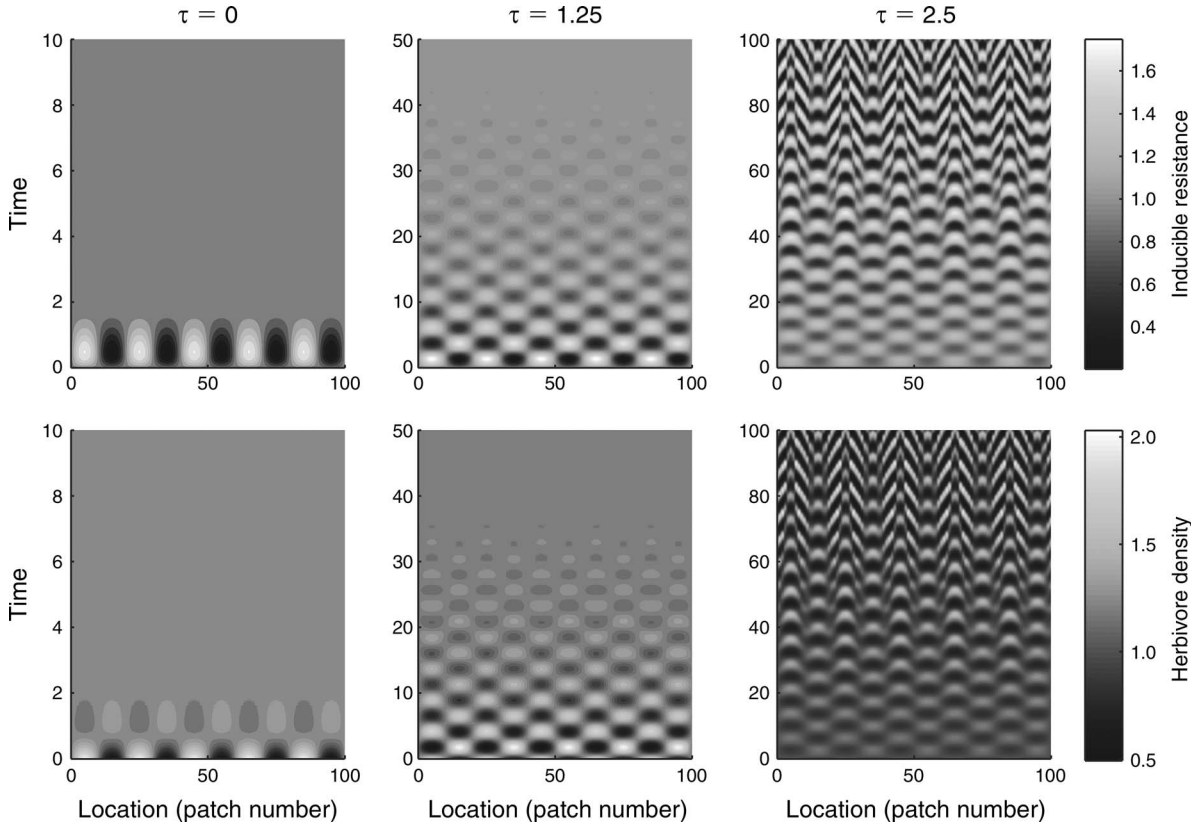

FIG. 2. Examples of spatiotemporal dynamics exhibited by the OBE model with different time delays (τ) in the onset of induction. Dynamics were obtained via numerical simulation of the full nonlinear model over 100 patches with periodic boundary conditions. Each location represents a patch. In each example, herbivores have an initial density that varies across patches as a sine wave with a spatial frequency $k = 0.314$, which corresponds to a spatial wavelength of 20 patches. Inducible resistance is at its uniform steady state. The scale of the time axis varies among scenarios for presentation purposes. Other parameter values are $\gamma = 0.25$, $\chi = 30.0$, $D = 12.0$, $b = 1.0$, and $\theta = 5.0$.

Increases in both the half-saturation constant b and the shape constant θ decrease the stability of the system (Fig. 3b). Recall that b is scaled relative to the equilibrium average herbivore density $\bar{H}^*$. When b is much less than 1.0, the induction response begins saturating below the average herbivore density, damping destabilizing swings in induction levels. When b is larger, herbivores must aggregate above their average density to bring about a large induction response, facilitating spatial pattern formation. This effect is greatly enhanced when θ is large and, consequently, the sigmoidal induction response has a steeper inflection. This steepness creates a threshold effect, where large numbers of herbivores build up in a patch before triggering large levels of resistance. Having a sigmoidal shape, where $\theta > 1$, is in fact necessary for instability to form. A necessary (but not sufficient) mathematical condition for instability (Appendix B) is

$$\frac{\theta b^{\theta}}{1 + b^{\theta}} > 1. \tag{6}$$

When $\theta = 1$, the induction response decelerates monotonically, and the inequality is never satisfied in this circumstance.

High background mortality m has a stabilizing effect (Fig. 3c), as it removes individuals at a rate not linked to the local induction level. Since the per capita rate m is constant, a higher total number of herbivores will die in high-density patches compared to lower density ones, making it difficult for aggregations of herbivores to be sustained. As mortality increases, the stability of the system increases and the critical time delay increases. Mortality can eventually become high enough that the system cannot lose stability at any time delay.

OBME model

The behavior of the OBME model is quite similar to that of the OBE model. As with the OBE model, a positive time delay ($\tau > 0$) and a sigmoidal induction response ($\theta > 1$) are required for stability. In fact, parameters shared between the OBE and OBME models have qualitatively, and mostly quantitatively, similar effects on stability and resulting spatiotemporal dynam-

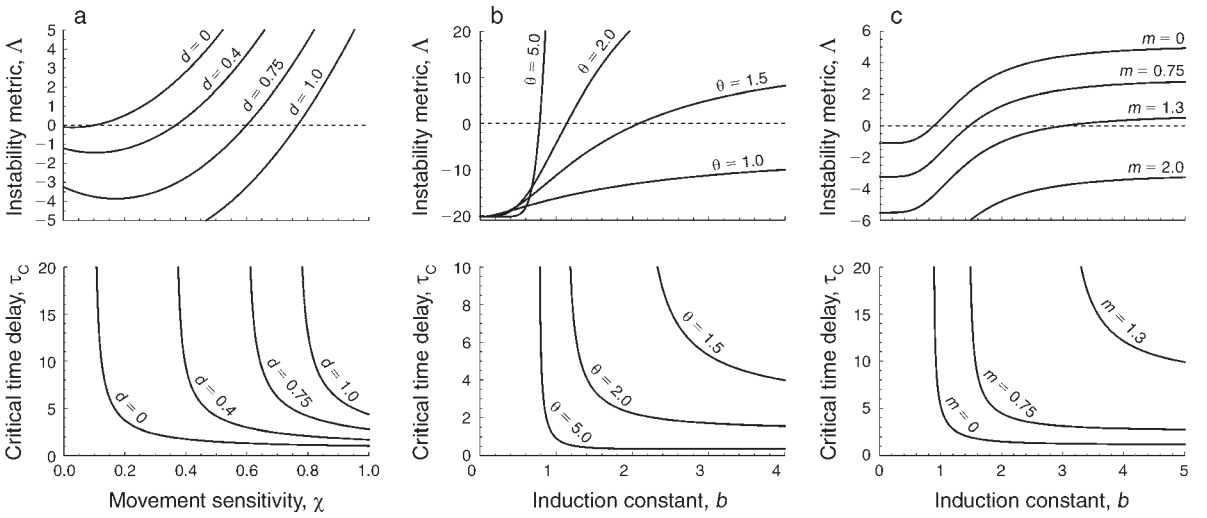

FIG. 3. Effects of parameter values on stability of the OBE model. The instability metric Λ from Eq. 5 is shown for different parameter combinations in the upper panels. This metric determines whether the model can lose stability and form spatial patterns when the time delay exceeds a critical value τ_C; positive values mean that such a critical time delay exists. The critical values of the time delay that lead to instability are given in the lower panels for each parameter combination. In panel (a), the baseline herbivore movement rate d and sensitivity of that rate on inducible resistance χ are varied; other parameter values used are $m = 0.3$, $b = 1.0$, $\theta = 5.0$, and $k = 2.0$. In panel (b), the induction half-saturation constant b and shape parameter θ are varied; other parameter values used are $m = 0.3$, $\chi = 2.0$, $D = 0.1$, and $k = 2.0$. There is no curve for τ_C when $\theta = 1.0$ since the model is always stable with this parameter combination regardless of the time delay. In panel (c), the induction half-saturation constant b and the herbivore mortality rate m are varied; other parameter values used are $\chi = 2.0$, $D = 0.1$, $\theta = 2.5$, and $k = 1.0$. There is no curve for τ_C when $m = 2.0$ since the model is always stable with this parameter combination regardless of the time delay.

ics. Following similar steps as those outlined in Appendix B for the OBE model, we find that the OBME can become unstable above some time delay τ_C when

$$\Lambda = \frac{\theta b^{\theta}}{1 + b^{\theta}} - \frac{dk^2}{2\beta + \chi k^2} - 1 \geq 0. \qquad (7)$$

Because of this overlap, we focus our exploration of the OBME on qualitative differences that arise from the functional dependence of herbivore mortality on inducible resistance.

A novel feature of the OBME model is that it can become unstable in response to uniform ($k = 0$) perturbations (Appendix C: Fig. C1). Under large ranges of parameter values, and when the time delay is very small, the relationship between stability, time delays, and the spatial frequency k of the perturbation are quite similar in the OBE and OBME models. Like the OBE model, the OBME model is stable for very small time delays, and as the time delay increases, small spatial-scale (large k) perturbations are the first to exhibit instability (c.f. Figs. 1 and 4). The range of unstable perturbation frequencies increases with increasing time delay. Unlike the OBE model, however, this expanding range eventually includes the full range of spatial frequencies, including $k = 0$. In fact, the perturbation growth rate ξ often becomes increasingly similar for all spatial frequencies with very large time delays, meaning that both small-scale and large-scale variation may contribute to long-term spatial patterns.

The broader ranges of spatial frequency that can become unstable in the OBME model result from the destabilizing effect of the herbivore mortality parameter β (Fig. 5). Rather than having a constant per capita value, mortality in the OBME model is tied to local

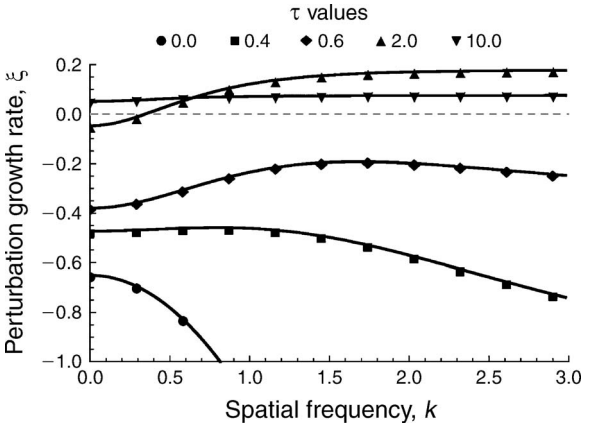

FIG. 4. The effect of the spatial frequency of an initial perturbation k and the induction time delay τ on the stability of the OBME (open behavioral and mortality effect) model, Eq. 3, as determined by the perturbation growth rate ξ. Other parameter values are $\beta = 0.3$, $\chi = 2.0$, $D = 0.1$, $b = 1.0$, and $\theta = 5.0$.

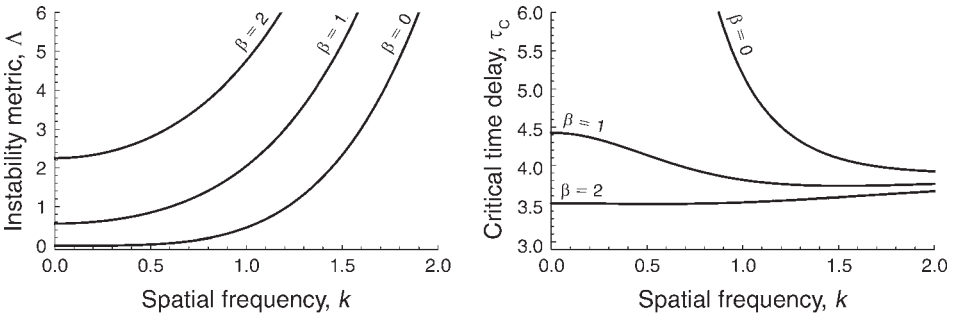

FIG. 5. Stability of the OBME model as influenced by the scaled mortality rate β. The instability metric is determined by Eq. 7. Other parameter values are $\chi = 2.0$, $D = 0.1$, $b = 1.0$, and $\theta = 2.5$.

induction, meaning that it can respond to variation in resistance levels. Mortality in the OBME model also influences the time delay required for instability: increases in β reduce τ_C, especially for small values of k. When β is small, large spatial frequencies (small spatial scales) are the first to become destabilized as the time delay is increased. Yet when β is large, this pattern is reversed, with small frequencies (large spatial scales) being the first to become unstable. The dominant effect of induction therefore shifts from movement responses to demographic ones with an increasing mortality effect β, leading to oscillations that are synchronized across all patches.

LBME model

The stability consequences of herbivore demographic and dispersal responses to induction that emerged in the OBME model are also apparent in the LBME model. The LBME can become unstable above some time delay τ_C when

$$\Lambda = \frac{\theta^2 b^{2\theta}}{(1+b^{\theta})^2} - \frac{\left(2(r-\beta)+(D+\chi)k^2\right)^2}{(2\beta+\chi k^2)^2} \geq 0. \qquad (8)$$

Large-scale perturbations can lead to instability, with global ($k = 0$) oscillations that are synchronized across patches being more likely with large time delays (Fig. 6). In contrast to the open recruitment models, the relationship between ξ and k tends to be unimodal rather than monotonic over a broad range of parameters and time delays. The hump-shaped relationship emerges in the LBME model when local demographic effects and movement effects reinforce each other at intermediate scales of k, leading to stronger tendency towards pattern formation.

In the LBME model, the mortality parameter β is strongly destabilizing, as in OBME model. Large values of β lead to instability over broad ranges of other parameters and reduce the time delay required for instability (Fig. 7a, b). The demographic effects of induction can be quite strong relative to open recruitment models because births as well as deaths are local. Even though only mortality is influenced by induction, local births appear to have more potential for causing demographically driven oscillations. For large-scale and especially global perturbations, increases in the growth rate, r, are destabilizing when r is small and stabilizing when r is large (Fig. 7a). A small amount of local population growth can intensify demographically driven oscillations because it promotes strong feedbacks between induction and herbivore dynamics. However, increases in r also increase the strength of herbivore self-regulation Eq. 4, which is a stabilizing force. This effect is especially strong when the perturbation scale is small; here, increases in r are almost always stabilizing (Fig. 7b).

A major difference between the LBME model and the previous open-recruitment models is that a sigmoidal induction response ($\theta > 1$) is no longer required for instability. Fig. 7c presents an example where $\theta = 1$ (a saturating response) is part of an unstable parameter combination with large b and a large time delay. For these parameter values, the strong feedbacks between induction and herbivore demographic processes are

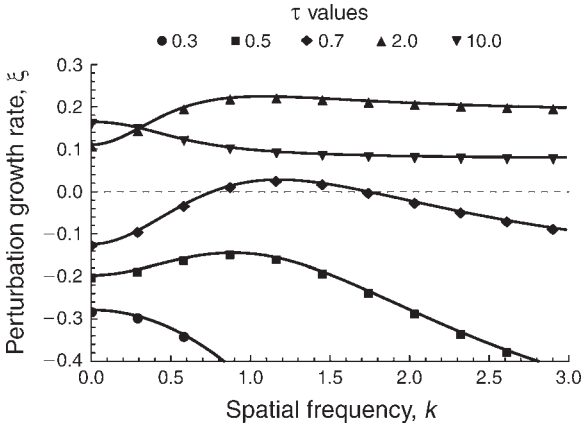

FIG. 6. The effect of the spatial frequency of initial perturbation k and the induction time delay τ on the stability of the LBME (local behavioral and mortality effect) model, Eq. 4, as determined by the perturbation growth rate ξ. Other parameter values are $\beta = 0.3$, $r = 0.1$, $\chi = 3.0$, $D = 0.1$, $b = 1.0$, and $\theta = 5.0$.

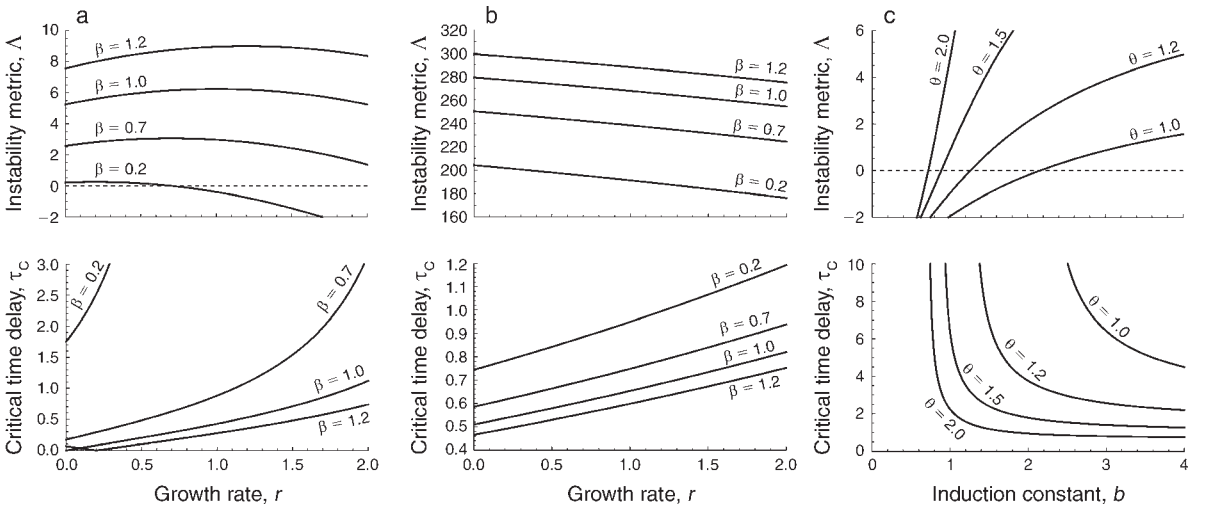

FIG. 7. Effects of parameter values on stability of the LBME model. The instability metric is determined by Eq. 8. In panel (a), the per capita herbivore growth rate r and the per capita mortality rate β are varied assuming a global ($k = 0$) perturbation; other parameter values used are $\chi = 3.0$, $D = 0.1$, $b = 1.0$, and $\theta = 5.0$. The same parameters are varied in panel (b) assuming a smaller scale perturbation where $k = 2.0$. In panel (c), the induction half-saturation constant b and shape parameter θ are varied; other parameter values used are $\beta = 2.0$, $r = 3.0$, $\chi = 2.0$, $D = 0.1$, and $k = 1.0$.

enough to lead to instability; no local buildup of herbivores moving away from regions of high induction, generated by thresholds, is required (Appendix C: Fig. C2).

Discussion

The question of how consumers distribute themselves among resource patches, potentially leading to local aggregations, is a longstanding focus in ecology. For herbivores, changes in plant quality, including inducible resistance, are cited as a potential aggregating mechanism. Yet, there is little work to date exploring the range of specific conditions where dynamic changes in plant quality can drive herbivore aggregation. We examined spatially explicit models of inducible resistance and herbivore population dynamics to explore how realistic features of resistance and different potential mechanisms of herbivore response influence spatial patterning. Both transient and persistent spatial patterns in resistance levels and herbivore densities developed in all models examined, where spatial patterns manifested as aggregations of herbivores that moved about in space. Except in very specific cases, spatial patterns arose when herbivores moved away from induced plants, there was a lag between herbivore damage and deployment of induced resistance, and the induction response had a sigmoid shape; all of these features have been observed in real plants and insects, for example, soybeans and Mexican bean beetles (Underwood 1999, 2000, Underwood et al. 2005), the stonecrop plant *Sedum lanceolatum* and *Parnassius smintheus* caterpillars (Roslin et al. 2008), and cotton bollworm caterpillars on *Arabidopsis thaliana* (Perkins et al. 2013). Herbivore movements and mortality occurring independent of induction tended to reduce spatial patterning. The mechanisms responsible for pattern formation listed above were evident regardless of the functional relationship between herbivore recruitment and mortality and induction in the model. However, in models where induction affected herbivore mortality, large-scale herbivore population cycles driven by the mortality response often co-occurred with smaller scale spatial patterns driven by herbivore movement. This increased the spatial scale over which herbivore aggregation is possible under many parameter combinations. When the effect of induction on mortality became dominant, however, spatial pattern formation was completely replaced by herbivore population cycles that were synchronized across space. This large-scale synchronization was most likely when herbivore recruitment was a function of local densities, and mirrors results seen in more complex models of insect population dynamics on forest trees that include inducible defenses (see references in Elderd et al. 2013). In these latter models, dispersal is somewhat limited over the large relevant scales (i.e., among forests), and induction may strongly influence recruitment and mortality of the focal forest Lepidoptera. Such features are less typical of smaller scale induction studies.

Previously, we identified the potential for aggregations to form in plant–herbivore systems with inducible resistance as a result of time delays (Underwood et al. 2005). Here, we presented a more rigorous examination of the mechanisms at work and the range of conditions under which spatial patterning can be expected, choosing functional forms reflecting realistic descriptions of plant defense responses. For example, Underwood (2010) found that two armyworm caterpillars (*Spodoptera exigua*) or 5% of leaf area damage on tomato plants was insufficient to generate a detectable response in herbivore growth or behavior. The effects of

leaf area damage on caterpillar growth also saturated after about 40%. Similar patterns of damage thresholds and saturation are also seemingly present in woody plants (Nykänen and Koricheva 2004) and plants in the family *Crassulaceae* (Roslin et al. 2008). The steepness of the transition between the threshold and saturation, as well as the damage level where this transition occurs relative to average damage levels, are key measurable parameters that determine stability (Eqs. 2–4). The ratio of the time delay in induction to induction's average decay time is also a critical measurable indicator of instability, and these values likely vary quite widely among systems. Consistent with our predictions, plants with long induction time delays appear to have the greatest negative effect on their herbivores (Nykänen and Koricheva 2004), although decay rates appear less well-characterized. In a small-scale field experiment, Underwood et al. (2005) found greater aggregation of beetles (*Epilachna verivestis*) among soybean genotypes with inducible resistance than among genotypes that were not inducible, generally in agreement with our model (see also Roslin et al. 2008). But while some measurements of different induction related parameters exist in the literature, more systematic descriptions are necessary for determining the potential for inducible defenses to drive herbivore aggregations and data on actual herbivore aggregation in the field is lacking even for systems where some parameter values are known.

In addition to the mechanisms described previously, the strength of stochasticity experienced in natural systems may influence whether spatial patterns predicted by our models emerge. For large populations like we model here, demographic and some forms of environmental stochasticity should lead to small-scale variation in herbivore densities that potentially acts to seed the development of spatial patterns. In addition, environmental and demographic stochasticity can drive aggregations and spatial patterning in models, even when they are stable in a deterministic sense (Wilson 1998, Butler and Goldenfeld 2009), or drive phase-locking and travelling waves (Blasius et al. 1999). The herbivore aggregations that we see in our models are likely susceptible to the influences of stochasticity. For example, strong transient spatial patterns can occur in our models even when deterministically stable (Fig. 2); these transient patterns could become persistent ones if the system is frequently perturbed by environmental or demographic stochasticity. In such a case, perturbations would continually re-excite transient dynamics, making patterns persist because they are never given enough time to settle towards equilibrium. This effect can lead to the formation of spatial patterns over a wider parameter range than predicted by our analyses of deterministic models. Nevertheless, the relationship between the spatial frequency of perturbation and the perturbation growth rate is similar in both unstable and weakly stable parameter ranges (Figs. 1, 4, and 6). Therefore, we predict that transient patterns would generate herbivore aggregations over spatial scales similar to those predicted in unstable parameter regions. This would not necessarily be the case when subjected to spatially correlated environmental stochasticity, which could either intensify wave-like spatial patterning or destroy it depending on the scale over which environmental correlations decay. When the model is highly stable, our previous work suggests that we might expect random or statistically more uniform than random patterns in the field, even in the face of stochastic variation (Underwood et al. 2005). This, of course, is most relevant to cases where individual herbivores are numerous enough that their dynamics are not completely overwhelmed by demographic stochasticity, such as insects, invertebrate grazers, and small-bodied mammals. In the case of larger mammals, variation in plant quality could reinforce aggregation tendencies largely influenced by other mechanisms, such as antipredator defenses or sociality.

We did not include changes in plant biomass, making our study similar to most others that model inducible resistance. It has long been argued that large changes in plant biomass, and therefore food limitation, are unlikely to generate cycles in herbivore populations as biomass removal is usually insufficient in extent or duration (Hairston et al. 1960, Price et al. 1980, Boonstra et al. 1998). However, food limitation does influence a range of insect and small mammal herbivore demographic traits (e.g., Myers et al. 2011), and models of food limitation can generate insect population cycles, given realistic assumptions (Abbott and Dwyer 2007). Food limitation may interact non-additively when paired with inducible resistance, generating instability when neither factor can do so in isolation (Abbott et al. 2008). We anticipate that food limitation that is weak is most likely to enhance the spatial instability we have described here: too much defoliation will negate the effects of induction by removing all inducible biomass, while no food limitation is essentially the case we have modeled. Stronger food limitation may also drive additional herbivore dispersal. This dispersal would conceivably work in opposition to herbivore aggregation because it would lead to conspecific repulsion without the induction mechanisms that first allow herbivore build-up. Weak food limitation that we have considered here is likely realistic. Even though defoliation is more easily realized at small scales, high levels of damage may still not be pervasive because induction will cause herbivores to avoid or move away quickly because of changes in plant quality or take shorter meals (e.g., Barker et al. 1995; D. McNutt, *unpublished data*).

In addition to damage, plant biomass will change by growth and reproduction. Induction potential may vary depending on the age of plants or plant-parts (Karban and Baldwin 1997). We assume that our plant population varies in resistance levels only across space and is otherwise homogenous in induction potential. Small, morphologically simple annual plants most likely fit

these assumptions of our models at the most literal level (Reynolds et al. 2012, 2013). Plants with more defined stage structure could exhibit increased within-plant herbivore heterogeneity. However, this does not negate the possibility of aggregations forming over larger scales, especially if herbivores tend to move easily among individual plants. In fact, stage-structured variation could add to delays in induction following herbivory, increasing instability (Liu et al. 2012). In a spatial context, that means we could see increased potential for spatial patterning resulting from stage-structured induction given our other assumptions hold.

The tendency for spatial patterns to develop in our model has consequences for both the evolution of inducible defenses and the effects of these defenses on ecological communities. Plants in our model experience herbivores in waves when the system is unstable and therefore deploy resistance periodically. Situations where plants experience mobile herbivore aggregations and thus highly variable damage are analogous to those shown by previous work to favor the evolution of inducible defenses. In particular, induction should be favored over constitutive or no defense scenarios when defense costs are high, damage is variable and/or unpredictable, or variability itself is detrimental to herbivore performance (Karban and Baldwin 1997, Agrawal and Karban 1999, Zangerl 2003, Karban 2011). While it is difficult to imagine how inducible defenses would evolve to favor spatial patterns to develop per se, evolutionary tuning of the threshold, speed, magnitude, and longevity of the induction response (as well as various herbivore responses) could reinforce mechanisms leading to herbivore aggregation. Indirect influences of aggregated herbivores on the evolutionary context for induced resistance may also arise by altering interactions between plants and other herbivores (Karban 2011). Defenses may target some natural enemies, while making plants more susceptible to others (e.g., Thaler et al. 2002). Strong variation in insect densities and induction levels could also alter the foraging efficiency of insect natural enemies, which may respond to induced plant volatiles (Thaler 2002). In mammals, foraging behavior of predators and herbivore antipredator defenses may feed back on plant defenses, either altering or reinforcing defense expression (Ford et al. 2014). Therefore, spatial variation in induction and induction-driven aggregations of herbivores may generate spatial variation in plant quality with cascading community-wide consequences, for example (Viswanathan et al. 2005, 2008). Given that instability is a common outcome in models that include realistic features of inducible resistance, extensions that consider the broader evolutionary and community consequences of the variation that results are a fitting and exciting next step.

We have presented a novel mechanism of ecological pattern formation based on consumer-induced trait variation in a resource species and consumer behavioral responses to that variation, mediated by a time delay. The destabilizing tendency of time delays has long been appreciated. While most studies in physical and biological sciences have focused on delay effects in nonspatial models, it is little surprise that time delays can contribute to spatial pattern formation as well. Examples of spatial instabilities arising from time delays occur in physical systems (Bertram and Mikhailov 2001), gene regulation (Seirin Lee and Gaffney 2010), and ecological models (Diaz Rodrigues et al. 2012, Tian 2012, Xinze et al. 2013; but see Klepac et al. [2007] and Wall et al. [2013] for examples where time delays are stabilizing in spatial models). However, none of these involve the nonlinear diffusion mechanism reflecting consumer behavior that we describe here; such nonlinear movement has been recently implicated in spatial pattern formation in other ecological models (Anderson et al. 2012, Liu et al. 2013). Given the prevalence of biological time delays and adaptive movement, we argue that there is high potential for this combination of mechanisms to generate spatial variation in other ecological contexts.

Acknowledgments

We would like to thank the Inouye/Underwood lab groups, Maurizio Tomaiuolo, Richard Bertram, Larry Li, Quan-Xing Liu, and two anonymous reviewers for helpful comments and discussions. This study was funded in part by a USDA CSREES Postdoctoral Fellowship Award No. 2005-35302-1699 and an NSF Award No. DMS-1122726 to KEA, a USDA CSREES Award No. 2005-35302-16311 to NU, and an NSF Award No. DEB-0816838 to BID.

Literature Cited

Abbott, K. C., and G. Dwyer. 2007. Food limitation and insect outbreaks: complex dynamics in plant-herbivore models. Journal of Animal Ecology 76:1004–1014.

Abbott, K. C., W. F. Morris, and K. Gross. 2008. Simultaneous effects of food limitation and inducible resistance on herbivore population dynamics. Theoretical Population Biology 73:63–78.

Agrawal, A. A., and R. Karban. 1999. Why induced defenses may be favored over constitutive strategies in plants. Pages 45–61 *in* R. Tollrian and C. D. Harvell, editors. The ecology and evolution of inducible defenses. Princeton University Press, Princeton, New Jersey, USA.

Anderson, K. E., F. M. Hilker, and R. M. Nisbet. 2012. Directional biases and resource-dependence in dispersal generate spatial patterning in a consumer-producer model. Ecology Letters 15:209–217.

Barker, A. M., S. D. Wratten, and P. J. Edwards. 1995. Wound-induced changes in tomato leaves and their effects on the feeding patterns of larval lepidoptera. Oecologia 101:251–257.

Bergelson, J., S. Fowler, and S. Hartley. 1986. The effects of foliage damage on casebearing moth larvae, *Coleophora serratella*, feeding on birch. Ecological Entomology 11:241–250.

Bernays, E. A., and R. F. Chapman. 1994. Host-plant selection by phytophagous insects. Chapman & Hall, New York, New York, USA.

Bertram, M., and A. S. Mikhailov. 2001. Pattern formation in a surface chemical reaction with global delayed feedback. Physical Review E 63:0066102.

Blasius, B., A. Huppert, and L. Stone. 1999. Complex dynamics and phase synchronization in spatially extended ecological systems. Nature 399:354–359.

Boonstra, R., C. J. Krebs, and N. C. Stenseth. 1998. Population cycles in small mammals: the problem of explaining the low phase. Ecology 79:1479–1488.

Butler, T., and N. Goldenfeld. 2009. Robust ecological pattern formation induced by demographic noise. Physical Review E 80:030902.

Cipollini, D. F., J. W. Busch, K. A. Stowe, E. L. Simms, and J. Bergelson. 2003. Genetic variation and relationships of constitutive and herbivore-induced glucosinolates, trypsin inhibitors, and herbivore resistance in *Brassica rapa*. Journal of Chemical Ecology 29:285–302.

Diaz Rodrigues, L. A., D. C. Mistro, and S. Petrovskii. 2012. Pattern formation in a space- and time-discrete predator-prey system with a strong Allee effect. Theoretical Ecology 5:341–362.

Edelstein-Keshet, L., and M. D. Rausher. 1989. The effects of inducible plant defenses on herbivore populations. I. Mobile herbivores in continuous time. American Naturalist 133:787–810.

Edwards, P. J., and S. D. Wratten. 1983. Wound induced defenses in plants and their consequences for patterns of insect grazing. Oecologia 59:88–93.

Edwards, P. J., S. D. Wratten, and H. Cox. 1985. Wound-induced changes in the acceptability of tomato to larvae of *Spodoptera littoralis*: a laboratory bioassay. Ecological Entomology 10:155–158.

Elderd, B. D., B. J. Rehill, K. J. Haynes, and G. Dwyer. 2013. Induced plant defenses, host-pathogen interactions, and forest insect outbreaks. Proceedings of the National Academy of Sciences USA 110:14978–14983.

Ford, A. T., J. R. Goheen, T. O. Otieno, L. Bidner, L. A. Isbell, T. M. Palmer, D. Ward, R. Woodroffe, and R. M. Pringle. 2014. Large carnivores make savanna tree communities less thorny. Science 346:346–349.

Gomez, S., W. van Dijk, and J. F. Stuefer. 2010. Timing of induced resistance in a clonal plant network. Plant Biology 12:512–517.

Gurney, W. S. C., and R. M. Nisbet. 1998. Ecological dynamics. Oxford University Press, New York, New York, USA.

Hairston, N. G., F. E. Smith, and L. B. Slobodkin. 1960. Community structure, population control, and competition. American Naturalist 94:421–425.

Kallenbach, M., G. Bonaventure, P. A. Gilardoni, A. Wissgott, and I. T. Baldwin. 2012. Empoasca leafhoppers attack wild tobacco plants in a jasmonate-dependent manner and identify jasmonate mutants in natural populations. Proceedings of the National Academy of Sciences USA 109:E1548–E1557.

Kaplan, I., and R. F. Denno. 2007. Interspecific interactions in phytophagous insects revisited: a quantitative assessment of competition theory. Ecology Letters 10:977–994.

Kaplan, I., M. E. Lynch, G. P. Dively, and R. F. Denno. 2007. Leafhopper-induced plant resistance enhances predation risk in a phytophagous beetle. Oecologia 152:665–675.

Karban, R. 2011. The ecology and evolution of induced resistance against herbivores. Functional Ecology 25:339–347.

Karban, R., and I. T. Baldwin. 1997. Induced responses to herbivory. University of Chicago Press, Chicago, Illinois, USA.

Karban, R., K. Shiojiri, M. Huntzinger, and A. C. McCall. 2006. Damage-induced resistance in sagebrush: volatiles are key to intra- and interplant communication. Ecology 87:922–930.

Klepac, P., M. G. Neubert, and P. van den Driessche. 2007. Dispersal delays, predator-prey stability, and the paradox of enrichment. Theoretical Population Biology 71:436–444.

Liu, Q.-X., A. Doelman, V. Rottschäfer, M. de Jager, P. M. J. Herman, M. Rietkerk, and J. van de Koppel. 2013. Phase separation explains a new class of self-organized spatial patterns in ecological systems. Proceedings of the National Academy of Sciences USA 110:11905–11910.

Liu, R. S., S. A. Gourley, D. L. DeAngelis, and J. P. Bryant. 2012. Modeling the dynamics of woody plant-herbivore interactions with age-dependent toxicity. Journal of Mathematical Biology 65:521–552.

Long, J. D., R. S. Hamilton, and J. L. Mitchell. 2007. Asymmetric competition via induced resistance: specialist herbivores indirectly suppress generalist preference and populations. Ecology 88:1232–1240.

Lundberg, S., J. Jaremo, and P. Nilsson. 1994. Herbivory, inducible defense and population oscillations: a preliminary theoretical analysis. Oikos 71:537–540.

Massey, F. P., A. R. Ennos, and S. E. Hartley. 2007. Herbivore specific induction of silica-based plant defences. Oecologia 152:677–683.

Morris, W. F., and G. Dwyer. 1997. Population consequences of constitutive and inducible plant resistance: herbivore spatial spread. American Naturalist 149:1071–1090.

Murray, J. D. 2003. Mathematical biology. Third edition. Springer, New York, New York, USA.

Myers, J., J. Cory, J. Ericsson, and M. Tseng. 2011. The effect of food limitation on immunity factors and disease resistance in the western tent caterpillar. Oecologia 167:647–655.

Nykänen, H., and J. Koricheva. 2004. Damage-induced changes in woody plants and their effects on insect herbivore performance: a meta-analysis. Oikos 104:247–268.

Orians, C. M., J. Pomerleau, and R. Ricco. 2000. Vascular architecture generates fine scale variation in systemic induction of proteinase inhibitors in tomato. Journal of Chemical Ecology 26:471–485.

Perkins, L. E., B. W. Cribb, P. B. Brewer, J. Hanan, M. Grant, M. de Torres, and M. P. Zalucki. 2013. Generalist insects behave in a jasmonate-dependent manner on their host plants, leaving induced areas quickly and staying longer on distant parts. Proceedings of the Royal Society B 280: 20122646.

Poore, A. G. B., L. Gutow, J. F. Pantoja, F. Tala, D. J. Madariaga, and M. Thiel. 2014. Major consequences of minor damage: impacts of small grazers on fast-growing kelps. Oecologia 174:789–801.

Price, P. W., C. E. Bouton, P. Gross, B. A. McPheron, J. N. Thompson, and A. E. Weis. 1980. Interactions among three trophic levels: influence of plants on interactions between insect herbivores and natural enemies. Annual Review of Ecology and Systematics 11:41–65.

Reynolds, J. J. H., X. Lambin, F. P. Massey, S. Reidinger, J. A. Sherratt, M. J. Smith, A. White, and S. E. Hartley. 2012. Delayed induced silica defenses in grasses and their potential for destabilising herbivore population dynamics. Oecologia 170:445–456.

Reynolds, J. J. H., J. A. Sherratt, A. White, and X. Lambin. 2013. A comparison of the dynamical impact of seasonal mechanisms in a herbivore-plant defense system. Theoretical Ecology 6:225–239.

Roslin, T., H. Syrjala, J. Roland, P. J. Harrison, S. Fownes, and S. F. Matter. 2008. Caterpillars on the run: induced defences create spatial patterns in host plant damage. Ecography 31:335–347.

Sarfraz, R. M., J. S. Cory, and J. H. Myers. 2013. Life-history consequences and disease resistance of western tent caterpillars in response to localised, herbivore-induced changes in alder leaf quality. Ecological Entomology 38:61–67.

Seirin Lee, S., and E. A. Gaffney. 2010. Aberrant behaviours of reaction diffusion self-organisation models on growing domains in the presence of gene expression time delays. Bulletin of Mathematical Biology 72:2161–2179.

Silkstone, B. E. 1987. The consequences of leaf damage for subsequent insect grazing on birch (*Betula* spp.): a field experiment. Oecologia 74:149–152.

Stork, W., C. Diezel, R. Halitschke, I. Gális, and I. T. Baldwin. 2009. An ecological analysis of the herbivory-elicited JA burst and its metabolism: plant memory processes and predictions of the moving target model. PLoS ONE 4:e4697.

Thaler, J. S. 2002. Effect of jasmonate-induced plant responses on the natural enemies of herbivores. Journal of Animal Ecology 71:141–150.

Thaler, J. S., R. Karban, D. E. Ullman, K. Boege, and R. M. Bostock. 2002. Cross-talk between jasmonate and salicylate plant defense pathways: effects on several plant parasites. Oecologia 131:227–235.

Thaler, J. S., M. J. Stout, R. Karban, and S. S. Duffey. 2001. Jasmonate-mediated induced plant resistance affects a community of herbivores. Ecological Entomology 26:312–324.

Tian, C. 2012. Delay-driven spatial patterns in a plankton allelopathic system. Chaos 22:013129.

Tollrian, R., and C. D. Harvell. 1999. The ecology and evolution of inducible defenses. Princeton University Press, Princeton, New Jersey, USA.

Underwood, N. 1999. The influence of plant and herbivore characteristics on the interaction between induced resistance and herbivore population dynamics. American Naturalist 153:282–294.

Underwood, N. 2000. Density dependence in induced plant resistance to herbivore damage: threshold, strength and genetic variation. Oikos 89:295–300.

Underwood, N. 2010. Density dependence in insect performance within individual plants: induced resistance to *Spodoptera exigua* in tomato. Oikos 119:1993–1999.

Underwood, N. 2012. When herbivores come back: effects of repeated damage on induced resistance. Functional Ecology 26:1441–1449.

Underwood, N., K. Anderson, and B. D. Inouye. 2005. Induced vs. constitutive resistance and the spatial distribution of insect herbivores among plants. Ecology 86:594–602.

Underwood, N., and M. Rausher. 2002. Comparing the consequences of induced and constitutive plant resistance for herbivore population dynamics. American Naturalist 160: 20–30.

Viswanathan, D. V., G. McNickle, and J. S. Thaler. 2008. Heterogeneity of plant phenotypes caused by herbivore-specific induced responses influences the spatial distribution of herbivores. Ecological Entomology 33:86–94.

Viswanathan, D. V., A. J. T. Narwani, and J. S. Thaler. 2005. Specificity in induced plant responses shapes patterns of herbivore occurrence on *Solanum dulcamara*. Ecology 86: 886–896.

Wall, E., F. Guichard, and A. R. Humphries. 2013. Synchronization in ecological systems by weak dispersal coupling with time delay. Theoretical Ecology 6:405–418.

Walters, D. 2011. Plant defense: warding off attack by pathogens, herbivores and parasitic plants. First edition. Blackwell Publishers, Chichester, UK.

Wilson, W. G. 1998. Resolving discrepancies between deterministic population models and individual-based simulations. American Naturalist 151:116–134.

Xinze, L., W. Hailing, and W. Weiming. 2013. Delay-driven pattern formation in a reaction–diffusion predator–prey model incorporating a prey refuge. Journal of Statistical Mechanics: Theory and Experiment 2013:P04006.

Zangerl, A. R. 2003. Evolution of induced plant responses to herbivores. Basic and Applied Ecology 4:91–103.

Supplemental Material

Ecological Archives

Appendices A–C and the Supplement are available online: http://dx.doi.org/10.1890/14-1697.1.sm